Published in final edited form as:
Biomaterials. 2008 ; 29(24-25): 3461–3468.

Mesenchymal stem cell interaction with ultra smooth nanostructured diamond for wear resistant orthopaedic implants

William C. Clem[1,2], **Shafiul Chowdhury**[1,3], **Shane A. Catledge**[1,3], **Jeffrey J. Weimer**[4], **Faheem M. Shaikh**[5], **Kristin M. Hennessy**[5], **Valery V. Konovalov**[1,3], **Michael R. Hill**[1,2], **Alfred Waterfeld**[6], **Susan L. Bellis**[1,2,5,*], and **Yogesh K. Vohra**[1,3,*]

1 *Center for Nanoscale Materials and Biointegration, Birmingham, AL, 35294-1170*

2 *Department of Biomedical Engineering, University of Alabama at Birmingham, Birmingham, AL, 35294-4440*

3 *Department of Physics, University of Alabama at Birmingham, Birmingham, AL, 35294-1170*

4 *Department of Chemistry and Department of Chemical and Materials Engineering, University of Alabama at Huntsville, Huntsville, AL 35899*

5 *Department of Physiology and Biophysics, University of Alabama at Birmingham, Birmingham, AL 35294-0005*

6 *Department of Chemistry, University of Alabama, Tuscaloosa, AL, 35487*

Abstract

Ultra smooth nanostructured diamond (USND) can be applied to greatly increase the wear resistance of orthopaedic implants over conventional designs. Herein we describe surface modification techniques and cytocompatibility studies performed on this new material. We report that hydrogen (H) -terminated USND surfaces supported robust mesenchymal stem cell (MSC) adhesion and survival, while oxygen (O) and fluorine (F) -terminated surfaces resisted cell adhesion, indicating that USND can be modified to either promote or prevent cell/biomaterial interactions. Given the favorable cell response to H-terminated USND, this material was further compared with two commonly-used biocompatible metals, titanium alloy (Ti-6Al-4V) and cobalt chrome (CoCrMo). MSC adhesion and proliferation were significantly improved on USND compared with CoCrMo, although cell adhesion was greatest on Ti-6Al-4V. Comparable amounts of the proadhesive protein, fibronectin, were deposited from serum on the three substrates. Finally, MSCs were induced to undergo osteoblastic differentiation on the three materials, and deposition of a mineralized matrix was quantified. Similar amounts of mineral were deposited onto USND and CoCrMo, whereas mineral deposition was slightly higher on Ti-6Al-4V. When coupled with recently published wear studies, these *in vitro* results suggest that USND has the potential to reduce debris particle release from orthopaedic implants without compromising osseointegration.

*Corresponding authors: Susan L. Bellis, PhD, Dept. of Physiology and Biophysics, MCLM 982A, University of Alabama at Birmingham, Birmingham, AL 35294-0005, Phone: (205) 934-3441; Fax: (205) 975-9028, bellis@uab.edu, Yogesh K. Vohra, PhD, Dept. of Physics, CH310, University of Alabama at Birmingham, Birmingham, AL 35294-1170, Phone: (205) 934-6662; Fax: (205) 934-8009, ykvohra@uab.edu.

Keywords

Diamond; Mesenchymal stem cell; Biocompatibility; Surface treatment; Protein adsorption; Osseointegration

1. Introduction

Total joint replacement is an effective treatment for relieving pain and restoring range of motion. As long as implants are positioned correctly and infection is avoided, they will generally last for many years. However, current implants have a limited life-expectancy, and younger patients who receive them generally expect to endure revision surgeries to replace worn components. A primary problem with current designs is the generation of wear debris particles at the articulating surface that causes local pain and inflammation. Large debris are normally sequestered by fibrous tissue, while small debris is taken up by macrophages and multinucleated giant cells which may release cytokines that result in inflammation. This inflammation cascade damages surrounding bone, ultimately resulting in osteolysis, loosening, and implant failure.

The proposed solution for the problem of osteolysis caused by wear debris is to develop ultrahard materials for the articulating surfaces that are more wear resistant, which would reduce the number of debris particles generated. Efforts to improve the wear surfaces have primarily focused on a few materials with exceptional strength, toughness, and hardness: aluminum and zirconium oxides, titanium nitride, carbon nitride, diamond-like carbon (DLC), and diamond produced by chemical vapor deposition (CVD diamond).

In addition to the development of ultrahard materials, efforts are being made to reduce the surface roughness of the articulating components, since smooth surfaces should produce less wear compared to rougher surfaces. In commercial joint prostheses available today, the most common approach is to use a polished metallic CoCrMo surface or a smooth ceramic surface that articulates with a much softer polyethylene surface. The rationale is that with this set-up, almost all of the debris generated will be the softer polyethylene debris, which is fairly well tolerated when produced in small amounts. However, on examination of implants retrieved from revision surgeries, it is common to find that bone fragments or cement trapped in the bearing surface has caused large scratches in the metal surface. It is also common to see macroscopic metallic transfer to ceramic components. These scratches and metallic transfer are sharp regions that greatly accelerate the wear of the polyethylene and result in much more debris. While the most promising bearings may completely eliminate the polyethylene from the implant design, these designs also require the strongest film adhesion of the coating. For these reasons, a diamond-on-polyethylene bearing is attractive compared to conventional designs, although a diamond-on-diamond bearing remains the eventual goal.

In our laboratories, we have patented processes for producing ultra smooth diamond coatings for Ti-6Al-4V using microwave plasma assisted chemical vapor deposition (CVD). Our first process, developed in 1999, utilized $H_2/CH_4/N_2$ plasma to produce diamond with RMS roughness of 14 nm [1-3]. The nitrogen is responsible for minimizing the single crystal growth, so that nanoscale diamond grains are produced. More recently, we found that addition of helium into the plasma mixture further reduces the diamond grain size, with RMS roughness of 5 nm being achieved [4]. This smoother coating, which we refer to as ultra-smooth nanostructured diamond (USND), is expected to further reduce wear when employed at the articulating surface of joint implants. We have published wear-testing studies separately [5,6], and further wear tests are ongoing.

Diamond coatings additionally have the advantage of chemical inertness, high electrical resistivity, and impermeability that is expected to reduce the crevice corrosion that is commonly seen on conventional metallic implants. These properties have led many groups to consider carbon coatings for applications that require osseointegration. Extensive literature is available that describes the biocompatibility of some carbon-based hard materials, such as pyrolytic carbon and diamond-like carbon (DLC) (reviewed in [7-10]). However, the nature of the carbon forms used in almost all of the previous studies is either amorphous (with primarily sp^2 bonding) or turbostratic pyrolytic carbon (similar to graphite, but with disordered layer structure). In comparison to other carbon coatings, very few biocompatibility studies have been performed on diamond produced by chemical vapor deposition (CVD diamond).

One indicator of biomaterial performance in orthopaedic applications is the interaction of the material with osteogenic cells. In the current study, we evaluated the behavior of human mesenchymal stem cells (MSCs) on USND discs that were modified with H, O, or F surface treatments. After elucidating surface treatment effects on cytocompatibility, cellular responses to H-terminated USND were compared with responses to either CoCrMo or Ti-6Al-4V, two biocompatible metals currently utilized in most commercially available implant designs. Collectively, this investigation addresses the potential utility of USND versus conventional materials for implant fixation.

2. Materials and Methods

2.1 Fabrication of biomaterial substrates

Extra low interstitial Ti-6Al-4V sheets with 1 mm thickness were purchased from Robin Materials (Mountain View, CA). Seven millimeter diameter discs were punched from the sheet and were then polished to a root-mean-square (RMS) roughness of 6 nm using a mechanical polisher with SiC paper, followed by a chemical–mechanical polish with a 0.06 μm colloidal silica solution containing 10% hydrogen peroxide. The polished discs were cleaned by ultrasonic agitation in a series of detergent solution, methanol, acetone, and finally deionized water.

Sample CoCrMo (ASTM F75) discs with 7 mm diameter were obtained from Smith & Nephew (Memphis, TN) and polished to an RMS roughness of 4 nm using a mechanical polisher with SiC paper, followed by a 3 μm and 1 μm diamond slurry solution. The polished disks were cleaned by ultrasonic agitation in a series of detergent solution, methanol, acetone, and finally deionized water.

The USND was deposited onto polished Ti-6Al-4V discs by a patent-pending process described in [11]. Briefly, cleaned and polished Ti-6Al-4V substrates were placed in a Wavemat® microwave-powered CVD reactor, equipped with a 6 kW, 2.4 GHz microwave generator. Base pressure before deposition was 15 mtorr. USND was deposited using a gas mixture of 87 sccm H_2, 36 sccm CH_4, 14.4 sccm N_2, and 213 sccm He at 0.91 kW power and a chamber pressure of 65 Torr. The surface temperature was maintained at 700°C for 4 hours before switching to a 10 min gradual cool down under a 100% hydrogen plasma. This process produces an USND coating with average grain size of 5 nm. Characterization by nanoindentation, Raman spectroscopy, x-ray diffraction (XRD), and atomic force microscopy (AFM) confirmed that the USND coatings produced for this study were consistent with previously published results obtained by this process [5,12].

2.2 Surface modification of USND

The surface atoms of the USND coating were replaced with either H, O, or F. Immediately following film deposition in the CVD reactor, the standard practice for our previous studies

has been to slowly cool the sample in a 100% hydrogen plasma by gradually reducing the microwave power over a 10-min period. This practice produces a H-terminated USND lattice that is very hydrophobic. A 10-min treatment with plasma composed of 10 sccm O_2 and 100 sccm He at 450°C produces an O-terminated USND lattice that is very hydrophilic. Additionally, F-terminated USND (hydrophobic) was produced by introducing F_2 gas into a closed chamber containing the H-terminated USND films for 48 hours at 100°C. These surface termination states were confirmed by x-ray photoelectron spectroscopy (XPS).

2.3 Surface analysis by XPS, AFM, and water contact angle

Elemental composition of the surface atoms was determined from XPS measurements on H-terminated USND, O-terminated USND, and F-terminated USND. Spectra for the F-terminated sample were obtained at a 90° take-off angle using a Kratos Axis 165 system (Kratos Analytical, Chesnut Ridge, NY) and monochromatic Al Kα x-rays at 210 W (14 kV, 15 mA). A charge neutralizer at a nominal bias of -1.15 V was used to compensate for peak shifting. Pass energies of 80 eV and 20 eV were used for survey and high-resolution scans, respectively. Spectra from the other two samples were obtained at 90° take-off angle using a Kratos XSAM 800 system with Mg Kα x-rays at 225 W (15 kV, 15 mA) and with the same pass energies. Compositional information was taken from survey and high-resolution via standard calculations that involve peak areas and component sensitivity factors.

The RMS roughness was measured on 2 × 2 μm scan areas by AFM (TopoMetrix Explorer). Surface wettability of the substrates was determined by the half angle method using a CAM-MICRO model contact angle meter (Tantec Inc., Schaumburg, IL), with deionized water as the probe liquid. Two spots were measured from each of the three samples and averaged.

2.4 Isolation and culture of MSCs

Human mesenchymal stem cells (MSCs) were isolated from bone marrow donations, as previously described [13]. Briefly, cells were pelleted by centrifugation, resuspended in Dulbecco's Modified Eagle Medium (DMEM), and then applied to a Histopaque-1077 column (Sigma, St. Louis, MO). A density gradient was generated by centrifugation at 500 *g* for 30 min. Cells from the DMEM/Histopaque interface were extracted with a syringe and seeded onto tissue culture dishes and cultured in DMEM containing 10% fetal bovine serum. Cells had a homogenous and fibroblast-like appearance, and no osteoclasts or adipocytes were present, as measured by Tartrate Resistant Acid Phosphatase (TRAP) and Oil-O-red staining, respectively. Bone marrow samples were obtained with prior approval from the University of Alabama Institutional Review Board.

2.5 Microscopic analysis of MSC morphology

As a first assessment of cytocompatibility of USND with hydrogen, oxygen, or fluorine surface treatments, MSC morphology was evaluated following 1 hour culture by reflected light microscopy. Mesenchymal stem cells were seeded at a density of 5×10^4 MSCs/disc onto H, O, or F-terminated USND discs and cultured in serum-free DMEM at 37°C for 1 h. Unattached cells were removed by washing with PBS. Digital images of the discs were taken following fixation in 3.7% formaldehyde, using reflected light microscopy (Fisher Micromaster light microscope equipped with top-mounted light source, objective lens, and digital camera). Cells could be visualized without staining on the highly polished surfaces.

Scanning electron microscopy (SEM) images were taken in order to observe the spread morphology observed on the H-terminated USND surface. For these images, MSCs were cultured for 24h, rinsed with PBS to remove unattached cells, and fixed in 2.5% glutaraldehyde in PBS. The attached cells were dehydrated in a gradient of ethanol in water, followed by a gradient of hexamethyldisilazane (HMDS) in ethanol, and then sputter coated with Au/Pd for

imaging. Images were obtained using a Philips 515 SEM with an accelerating voltage of 10 kV.

Fluorescent images were taken to observe the morphology of MSCs cultured for extended times on H-terminated USND. Mesenchymal stem cells were seeded at a density of 5×10^4 cells/disc onto H-terminated USND and cultured in DMEM + 10% FBS at 37°C for 1 h, 24 h, 7 days, and 14 days. Unattached cells were removed by washing with PBS, and attached cells were fixed in 4% formaldehyde in PBS. Cells were treated with 0.2% Triton-X 100 (Sigma T9284) in PBS, blocked in 2% denatured bovine serum albumin (dBSA), and probed for actin with Alexa 488-phalloidin (Invitrogen A12379, 1:200) in 25 mM Tris buffer containing 2% dBSA for 45 min at 37°C. Nuclei were labeled with 20 μg/mL DAPI (Invitrogen D21490) in PBS for 4 min at room temp, followed by rinsing in Tris-buffer. Fluorescent images were taken with an 80i Nikon Eclipse microscope.

2.6 MSC adhesion assays

Adhesion of MSCs to H-terminated USND was compared to Ti-6Al-4V and CoCrMo. Three samples of each material were coated with fetal bovine serum overnight at 4°C, and three samples of each were left uncoated. Following serum coating, samples were washed with PBS to remove loosely-bound proteins. Mesenchymal stem cells were added at a concentration of 5×10^4 cells/disc in serum-free DMEM and allowed to adhere for 90 min at 37°C. Unattached cells were then removed by three washes with phosphate-buffered saline (PBS) on a mechanical shaker. Attached cells were lysed by ultrasonic agitation in 10 mM Tris, 1 mM EDTA buffer at pH 8 (TE buffer) containing 1% Triton X-100. The DNA content of the attached cells was assayed by addition of Picogreen reagent (Molecular Probes) according to manufacturer's protocol. Absorbance was read on a spectrometer at 612nm, compared to a DNA standard curve, and normalized to CoCrMo. Two independent experiments were performed, with each surface tested in triplicate.

2.7 Fibronectin adsorption assay

The Ti-6Al-4V, CoCrMo, and H-terminated USND discs were coated with fetal bovine serum (FBS) overnight at 4°C. They were washed twice with PBS to remove unattached proteins. The remaining proteins adsorbed to the surfaces were removed by shaking for 5 min in 100 μL of boiling 25 mM Tris buffer containing 5% 2-mercaptoethanol and 20% SDS. Gel loading on each lane was on an equal volume basis, with 50 μL/lane of each desorbed protein solution resolved on a 6% polyacrylamide gel. For western blot analyses, proteins were transferred to PVDF membrane, blocked in 5% dry milk, and probed with polyclonal anti-fibronectin primary antibody (Chemicon AB1954, 1:2000), followed by an HRP-conjugated secondary antibody (ECL NA9340V, 1:2000). Proteins were detected by enhanced chemiluminescence (Immobilon, Milipore, Billerica, MA).

2.8 MSC proliferation assays

Proliferation of MSCs on H-terminated USND was compared to Ti-6Al-4V and CoCrMo. Mesenchymal stem cells were seeded at low density (7,500 cells/disc) and cultured in DMEM containing 10% FBS. After 3 days or 7 days of culture, the media was replaced with 200 μL of DMEM (free of phenol red) containing 100 μg MTT. The viable cells were allowed to convert the MTT to formazan for 4 hours before lysing cells with SDS in 0.01 M HCl. Absorbance of formazan was read on a spectrometer at 570 nm and normalized to CoCrMo. Two independent experiments were performed, with each surface tested in triplicate.

2.9 Quantifying the deposition of mineralized matrix

MSCs were added at a high density (5×10^4 cells) to USND, Ti-6Al-4V and CoCrMo discs, and were cultured for two days in DMEM containing 10% FBS to form a confluent cell layer on the surface. The media was then replaced every 2–3 days with an osteogenic media (except for the negative control) composed of DMEM + 10% FBS, supplemented with 0.05 mM aspartic acid, 10 mM 2-glycerolphosphate, and 100 nM dexamethasone. A mineralized matrix could begin to be visualized on the highly polished surfaces at approximately 3 weeks (data not shown). After 4 weeks, cells were lysed and the mineralized matrix was solubilized by shaking for 24 h in 0.5 M HCl. Supernatants were analyzed for calcium by addition of phenolsulphonephthalein dye (Quantichrom, Bioassay Systems, Hayward, CA), which forms a stable blue colored complex specifically with free calcium. The intensity of the color, measured at 612 nm, was compared to a $CaCl_2$ standard curve and normalized to CoCrMo. Three independent experiments were performed, with each surface tested in triplicate.

2.10 Statistical Analysis

Data sets were assessed using one-way ANOVA. If significant differences were found, Fisher's Protected Least Significant Differences post hoc test was used to determine the level of significance. A 95% confidence level was considered significant.

3. Results

3.1 Surface Analysis

The surface layer of an implant determines essentially the biocompatibility whereas the bulk material imparts its mechanical properties. In the current study USND, Ti-6Al-4V, and CoCrMo substrates were polished to a mirror finish in an attempt to minimize differences in topography between samples. The RMS roughness of all samples was very similar; the RMS values were 6 nm for Ti-6Al-4V, 4 nm for CoCrMo, and 5 nm for USND.

Samples were also analyzed by XPS, which reveals the atomic concentrations of elements in the topmost 10 nm of the surface. The XPS survey scans from H-terminated, F-terminated and O-terminated USND are shown in Figure 1. Compositional ratios for O/C and F/C calculated from these spectra are given in Table 1. The increases in O/C and F/C, when compared to the values from the H-treated sample, represent a direct increase in the surface number density of oxygen or fluorine atoms respectively. The H-terminated and O-terminated samples showed Si peaks, while the F-terminated samples showed S peaks. Component fits were also done on high resolution scans of the C 1s and O 1s peaks for each sample (not shown). The ratio of hydroxyl to carbonate oxygen and carbonyl to aliphatic carbon were determined from these fits and are included in Table 1. With O-treatment, the hydroxyl to carbonate and carbonyl to aliphatic ratios increase. With F-treatment, the hydroxyl to carbonate ratio increases but the carbonyl to aliphatic ratio decreases. Finally, water contact angles were measured for representative samples, and it was found that values for H and F terminated substrates were very similar, and both of these materials were significantly more hydrophobic than O-terminated substrates (see Table 1).

3.2 Analysis of surface treatments on MSCs

When cells attach to endogenous extracellular matrices, they reorganize their actin cytoskeleton, adopting a spread morphology. This event is necessary for the survival of most adherent cell types, and is also important for the osteoblastic differentiation of MSCs. As a preliminary evaluation of the cytocompatibility of USND and each of the surface treatments, we examined the effect of the material on the morphology of mesenchymal stem cells. Considerable differences between the surface treatments were apparent, even after very short

time in culture. After 1-hour culture, numerous cells had adhered to the H-terminated samples (Figure 2, panel a), and the cells had adopted a well-spread morphology, with pseudopodia extending along the biomaterial surface (Figure 3). In contrast, no cells attached to the F-terminated samples (Figure 2, panel c). On O-terminated samples, a limited number of very rounded cells was apparent (Figure 2, panel b), however all the cells could be dislodged by gentle agitation (not shown), indicating that attachment was very weak.

At longer culture times, no cells adhered or survived on O-terminated or F-terminated USND surfaces, and therefore cell behavior on these surfaces was not studied further. However, the H-terminated USND surfaces consistently supported adhesion and spreading of MSCs at multiple time points ranging from 3 hours to 14 days (Figure 4). During this time interval, cell number increased until a confluent layer had covered the surface, indicating that the MSCs were proliferating. In light of the favorable cell response to H-terminated USND, our subsequent experiments focused on comparing MSC behavior on H-terminated USND with cell behavior on Ti-6Al-4V and CoCrMo, given that these latter materials are known to be biocompatible.

3.3 MSC adhesion

Attachment of MSCs to the surface of the biomaterial is a critical early step in the osseointegration of an implant. Since MSCs appeared to strongly bind to H-terminated USND in our initial evaluation, a quantitative analysis of MSC adhesion was performed and compared to Ti-6Al-4V and CoCrMo. To this end, we examined MSC adhesion on material surfaces without serum, and on substrates pre-coated with serum (FBS). As shown in Figure 5, cell adhesion to USND is increased in comparison to cobalt chrome, although adhesion to titanium alloy was found to be highest, whether in the presence of serum or in serum-free conditions. Interestingly, cell adhesion to the substrates not coated with serum was only slightly lower than that noted on surfaces coated with serum, suggesting that cells bind well to these biomaterials in the absence of adsorbed extracellular matrix molecules.

3.4 Fibronectin adsorption

The biocompatibility of implant materials depends, in part, upon the capacity of the material surface to adsorb endogenous proteins that regulate cell behavior. Pro-adhesive proteins, such as fibronectin, are abundant in blood and may play an important role in mediating cell/biomaterial interactions by providing integrin binding sites for cell adhesion [14]. Accordingly, we coated Ti-6Al-4V, CoCrMo, and H-terminated USND with serum, and then used Western blots analysis to determine the amount of fibronectin deposited on the material surface (Figure 6). We found that the amount of fibronectin associated with USND compares very closely with that of Ti-6Al-4V and CoCrMo.

3.5 MSC proliferation

Fluorescent images of adherent cells (Figure 4) suggested that cells were proliferating on the USND surfaces, however in order to quantify cell proliferation, MTT assays were performed (Figure 7). These experiments revealed that at 7 days following cell seeding, there was a similar number of viable cells on H-terminated USND and Ti-6Al-4V surfaces, with a significantly lower cell number on CoCrMo. Further studies are needed to determine whether the lower cell number observed on CoCrMo is due to a slower rate of proliferation, or to reduced cell survival, or both.

3.6 Deposition of mineralized matrix

Orthopaedic biomaterials should encourage the attachment and proliferation of MSCs; however, these are only the first steps in the process of osseointegration. Stem cells must also

be capable of differentiating into osteoblasts that ultimately produce a mineralized matrix on the surface of the biomaterial. In order to induce osteoblastic differentiation, MSCs were seeded onto the material substrates, and then grown in osteogenic media (OS+) for 4 weeks. The resulting mineral layer deposited by cells was solubilized, and the calcium content was quantified (Figure 8). As a control, cells were also grown on tissue culture plastic in the presence or absence of osteogenic media. As shown, cells grown on tissue culture plastic in osteogenic media deposited a calcium-rich matrix, whereas only negligible amounts of calcium were apparent in the cultures of cells grown in the absence of osteogenic media (normal growth media), confirming that cells had undergone differentiation. Quantification of calcium content for the cultures on metal substrates showed that similar amounts of mineralized matrix were deposited by the cells onto USND and cobalt chrome, while a slight increase in mineral deposition was observed for titanium alloy.

4. Discussion

In the past, CVD diamond has undergone little biocompatibility testing, and it has been unclear whether the biological response to CVD diamond (which can be highly crystalline and sp^3 bonded) will relate to that of DLC (which is non-crystalline) or pyrolytic carbon (which is primarily sp^2 bonded). The purpose of this study was to evaluate *in vitro* responses of osteogenic cells, specifically, MSCs, with USND, our formulation of CVD diamond. Unlike DLC, which contains a high amount of hydrogen, the bulk of USND is nearly hydrogen-free, with mostly sp^3 carbon.

The literature describing cell adhesion and survival on CVD diamond has been highly mixed. Tang, *et. al.* were among the first to examine cellular response to CVD diamond, and their study revealed that neutrophil adhesion to CVD diamond was equivalent to stainless steel [15]. More recently, Popov, et. al., found that SaOS-2 cells (an osteoblast cell line) and LEP cells (human lung fibroblasts) survive for extended time periods on CVD diamond [16,17]. In contrast to the previous studies that concluded that CVD diamond can promote adhesion, there are several studies that concluded that CVD diamond does not support adhesion. Ariano, *et. al.* described very low survival rates (fewer than 10%) of neurons cultured on homoepitaxial CVD diamond, without pre-coating with a layer of laminin [18]. Two separate groups have both concluded recently that platelet aggregation is minimal on CVD diamond [19,20]. Finally, Jakubowski and Mitura concluded that CVD diamond resists bacterial colonization better than titanium or steel [21,22]. These highly variable results regarding cell interactions with CVD diamond may be due to phenotypic differences in the cell types studied, differences in surface treatments of CVD diamond, or both.

In our studies of MSCs, we found that cellular responses to USND depend greatly on the surface treatment, which may explain, in part, the variable results observed previously with diamond formulations. More specifically, cells adhered to, and proliferated, on H-terminated USND, but not on F or O-terminated USND. Physicochemical characterization of the various surface treatments suggested that, while MSCs clearly respond to their immediate surface chemistry, the hydrophobic / hydrophilic nature of the surface may be less critical for influencing cell behavior, at least for USND materials. The H-terminated and F-terminated surfaces had similar water contact angles, indicating a degree of hydrophobicity, but each surface was distinctly different in its topmost surface chemistry. Other than the enrichment of the surface with H, O, or F by plasma treatment, changes to functional groups on the surface may affect the cell response. With O-treatment, the hydroxyl to carbonate and carbonyl to aliphatic ratios increase. This observation is likely indicating that carbonate-type oxygen species are being depleted while hydroxyl and carbonyl species are being created. The strong hydrophilic nature of this surface, evidenced by a water contact angle of $< 2°$, is in agreement with this assertion. With F-treatment, the hydroxyl to carbonate ratio increases but the carbonyl to aliphatic ratio

decreases. This behavior is likely indicating that fluorine is substituting for both the carbonate and carbonyl oxygen atoms on the surface, leaving hydroxyl species unaffected. Further systematic studies of the observations might be useful to elucidate the extent to which both surface chemistry and wettability play a role in cell adhesion and growth.

The mechanism underlying the high degree of MSC adhesion to H-terminated, but not F or O-terminated, USND is presently unknown. One possibility may relate to the intrinsic surface conductive properties of H-terminated surfaces [23–25]. MSCs are an anchorage-dependent cell type that are known to initiate apoptosis when they fail to attach to a substrate [26], so inability to attach can limit cell survival. One of the goals of the current study was to identify a surface treatment that would encourage osseointegration, therefore a major focus of this investigation was to compare cell behavior on H-terminated USND with two commonly used biocompatible alloys, Ti-6Al-4V and CoCrMo. However, the ability to tightly control cell adhesion is very important, as there are biomedical applications for both inert and pro-adhesive surfaces. Our studies suggest that USND is a highly versatile material that can be modified to either promote or completely block cell adhesion. Future studies aimed at identifying the mechanism for lack of cell attachment to O and F- terminated surfaces may facilitate the development of novel medical devices or treatments.

Cellular response to biomaterials depends initially on the interaction of adhesion receptors with proteins adsorbed to the surface. Adsorbed proteins can be detected on biomaterials within a second of exposure to the blood, and a monolayer of adsorbed proteins forms in seconds to minutes [27]. Fibronectin, vitronectin, and fibrinogen are pro-adhesive proteins, with relatively high concentration in blood, that are recognized by various cellular integrins and platelet receptors. These plasma proteins play an important role in the initial recruitment of cells to the biomaterial surface [28]. Although protein adsorption has been reported to be influenced by surface energy and wettability [29], we observed similar amounts of fibronectin adsorbed to the very hydrophobic surface of H-terminated USND as was adsorbed to Ti-6Al-4V and CoCrMo. Previous reports in the literature concerning protein adsorption to CVD diamond have been variable. Tang, *et. al*, found that similar amounts of fibrinogen adsorb to CVD diamond and titanium [15], but Garguilo and Mitura reported less fibrinogen binding to CVD diamond compared to titanium [30] or steel [22]. While the total amount of adsorbed fibronectin in this study is similar, the effect of this hydrophobic surface on the conformation of adsorbed proteins remains to be tested. Ideally, the proteins should adsorb in a conformation that allows for the pro-adhesive motifs, such as RGD, to be accessible by MSC integrins.

A comparison of MSC attachment to H-terminated USND, CoCrMo, or Ti-6Al-4V revealed that USND supported greater cell adhesion than CoCrMo, although less than Ti-6Al-4V. The adhesion assays in this study were performed both with and without pre-coating the biomaterials with serum, prior to introducing cells. As expected, the adsorbed serum proteins increased adhesion on all surfaces. Interestingly, a significant amount of cell adhesion was noted on all surfaces, even in the absence of adsorbed proteins, and this adhesion was strong enough to endure agitation on a mechanical shaker. Adhesion of MSCs is generally very low in serum-free conditions on many biomaterials, including hydroxyapatite [31]. Thus, the finding that MSCs bind well to implant metals in the absence of adsorbed serum proteins suggests that there may be alternative adhesive mechanisms beyond integrin-dependent binding to traditional integrin ligands. Further studies of cell adhesion mechanisms are warranted, given that attachment of MSCs is a critical first step toward osseointegration.

Longer-term measurements of cell number (3–7 days) indicated that MSCs exhibited a similar degree of proliferation on USND and Ti-6Al-4V. In contrast, fewer viable cells were apparent on CoCrMo. Reduced cell number on CoCrMo may reflect a slower rate of proliferation, reduced cell survival on CoCrMo, or both. The biocompatibility of Ti-6Al-4V is considered

by most groups to be superior to CoCrMo [32], and adverse effects of cobalt [33], chromium [34], and molybdenum [35] on other cell types have been identified. CoCrMo alloy particles have been shown to be toxic to some degree, with cell death increasing as the particle dosage increases [36,37]. Our studies of MSC adhesion and proliferation suggest that USND is more cytocompatible than CoCrMo, and comparable to Ti-6Al-4V.

While MSC attachment and proliferation are critical early steps in the process of osseointegration of a biomaterial, the material should also support differentiation of stem cells along an osteoblastic lineage. Ultimately, firm fixation of an orthopaedic implant depends on deposition of a mineralized matrix directly on the surface of the implant by osteoblasts. We observed that there was only a slight increase in the amount of matrix mineralization by MSCs adherent to Ti-6Al-4V, whereas mineralization of H-terminated USND and CoCrMo surfaces was similar, indicating that the processes of osteoblastic differentiation and matrix mineralization readily occur on USND coatings. Despite some biocompatibility advantages of Ti-6Al-4V over CoCrMo, the relatively low hardness of Ti-6Al-4V precludes its use in many orthopaedic applications where wear-resistance is needed. Collectively, our results suggest that USND could be substituted in place of Ti-6Al-4V or CoCrMo when a wear-resistant surface is needed. USND's primary improvement is increased wear-resistance, with hardness improved 14-fold over Ti-6Al-4V and 7-fold over CoCrMo, and this advantage seems to occur without compromising cytocompatibility.

5. Conclusion

Results from the current study suggest that USND is a highly versatile material, which can either support or resist MSC adhesion, depending on the surface treatment. The ability to control cell adhesion is important, as there are biomedical applications for both inert and pro-adhesive surfaces. We further demonstrate that an H-terminated USND surface promotes cell adhesion and survival, fibronectin adsorption, proliferation, and osteoblastic differentiation, as evidenced by matrix mineralization. Although Ti-6Al-4V offers a slight improvement in adhesion and mineralization, the low hardness precludes the use of titanium alloys for many orthopaedic applications, and CoCrMo is often selected instead. USND offers some improvements in cytocompatibility over CoCrMo (adhesion and proliferation of MSCs), while hardness is improved 14-fold over Ti-6Al-4V and 7-fold over CoCrMo. When coupled with recently published wear studies [5,6], these *in vitro* results suggest that USND has the potential to reduce debris particle release of biomedical implants without compromising osseointegration, thus minimizing the possibility of implant loosening over time.

Acknowledgements

We acknowledge support from the National Institute of Dental and Craniofacial Research (NIDCR) under grant # R01DE013952 (YKV) and the National Institute of Arthritis and Musculoskeletal and Skin Diseases (NIAMS) under grant # R01AR51539 (SLB). WC Clem acknowledges support from the NIH training Grant Number T32EB004312 from the National Institute of Biomedical Imaging and Bioengineering (NIBIB). The content is solely the responsibility of the authors and does not necessarily represent the official views of the National Institutes of Health. The authors would like to thank Smith and Nephew Orthopaedics (Memphis, TN) for generously providing cobalt chrome samples and Albert Tousson and the High Resolution Imaging Facility at UAB for assistance in fluorescent imaging.

References

1. Catledge SA, Vohra YK. High density plasma processing of nanostructured diamond films on metals. Journal of Applied Physics 1998;84(11):6469.
2. Catledge SA, Vohra YK. Effect of nitrogen addition on the microstructure and mechanical properties of diamond films grown using high-methane concentrations. Journal of Applied Physics 1999;86(1): 698.

3. Catledge, SA.; Vohra, YK. Mechanical Properties of Structural Films. West Conschohocken, PA: ASTM; 2001.
4. Konovalov VV, Melo A, Catledge SA, Chowdhury S, Vohra YK. Ultra-smooth nanostructured diamond films deposited from He/H2/CH4/N2 microwave plasmas. J Nanosci Nanotechnol 2006;6 (1):258–61. [PubMed: 16573106]
5. Chowdhury S, Borham J, Catledge SA, Eberhardt AW, Johnson PS, Vohra YK. Synthesis and mechanical wear studies of ultra smooth nanostructured diamond (USND) coatings deposited by microwave plasma chemical vapor deposition with $He/H_2/CH_4/N_2$ mixtures. Diamond and Related Materials. 200710.1016/j.diamond.2007.08.041
6. Hill MR, Catledge SA, Konovalov V, Clem WC, Chowdhury SA, Etheridge BS, et al. Preliminary tribological evaluation of nanostructured diamond coatings against ultra-high molecular weight polyethylene. J Biomed Mater Res B Appl Biomater. 200710.1002/jbm.b.30926
7. Cui FZ, Li DJ. A review of investigations on biocompatibility of diamond-like carbon and carbon nitride films. Surface and Coatings Technology 2000;131:481–7.
8. Dearnaley G, Arps JH. Biomedical applications of diamond-like carbon (DLC) coatings: A review. Surface & Coatings Technology 2005;200(7):2518–24.
9. Grill A. Diamond-like carbon coatings as biocompatible materials-an overview. Diamond and Related Materials 2003;12:166–70.
10. Roy RK, Lee KR. Biomedical applications of diamond-like carbon coatings: A review. Journal of Biomedical Materials Research Part B 2007;83(1):72.
11. Konovalov VV, Vohra YK, Catledge SA. Ultra-smooth nanostructured diamond films and compositions and methods for producing same. #PCT/US2006/038222. 2007inventors
12. Chowdhury S, Hillman DA, Catledge SA, Konovalov VV, Vohra YK. Synthesis of ultrasmooth nanostructured diamond films by microwave plasma chemical vapor deposition using a $He/H_2/CH_4/N_2$ gas mixture. Journal of Materials Research 2006;21(10):2675–82.
13. Kilpadi KL, Sawyer AA, Prince CW, Chang PL, Bellis SL. Primary human marrow stromal cells and Saos-2 osteosarcoma cells use different mechanisms to adhere to hydroxylapatite. J Biomed Mater Res A 2004;68(2):273–85. [PubMed: 14704969]
14. Siebers MC, ter Brugge PJ, Walboomers XF, Jansen JA. Integrins as linker proteins between osteoblasts and bone replacing materials. A critical review Biomaterials 2005;26(2):137–46.
15. Tang L, Tsai C, Gerberich WW, Kruckeberg L, Kania DR. Biocompatibility of chemical-vapour-deposited diamond. Biomaterials 1995;16(6):483–8. [PubMed: 7654876]
16. Popov C, Kulisch W, Jelinek M, Bock A, Strnad J. Nanocrystalline diamond/amorphous carbon composite films for applications in tribology, optics and biomedicine. Thin Solid Films 2006;494(1–2):92–7.
17. Popov C, Kulisch W, Reithmaier JP, Dostalova T, Jelinek M, Anspach N, et al. Bioproperties of nanocrystalline diamond/amorphous carbon composite films. Diamond and Related Materials 2007;16:735–9.
18. Ariano P, Baldelli P, Carbone E, Gilardino A, Giudice AL, Lovisolo D, et al. Cellular adhesion and neuronal excitability on functionalised diamond surfaces. Diamond and Related Materials 2005;14:669–74.
19. Narayan RJ, Wei W, Jin C, Andara M, Agarwal A, Gerhardt RA, et al. Microstructural and biological properties of nanocrystalline diamond coatings. Diamond & Related Materials 2006;15(1112):1935–40.
20. Okroj W, Kaminska M, Klimek L, Szymanski W, Walkowiak B. Blood platelets in contact with nanocrystalline diamond surfaces. Diamond and Related Materials 2006;15:1535–9.
21. Jakubowski W, Bartosz G, Niedzielski P, Szymanski W, Walkowiak B. Nanocrystalline diamond surface is resistant to bacterial colonization. Diamond & Related Materials 2004;13(10):1761–3.
22. Mitura K, Niedzielski P, Bartosz G, Moll J, Walkowiak B, Pawlowska Z, et al. Interactions between carbon coatings and tissue. Surface and Coatings Technology 2006;201:2117–23.
23. Chakrapani V, Angus JC, Anderson AB, Wolter SD, Stoner BR, Sumanasekera GU. Charge Transfer Equilibria Between Diamond and an Aqueous Oxygen Electrochemical Redox Couple. Science 2007;318(5855):1424. [PubMed: 18048683]

24. Kawarada H. Hydrogen–terminated diamond surfaces and interfaces. Surface Science Reports 1996;26(7):205–59.
25. Maier F, Riedel M, Mantel B, Ristein J, Ley L. Origin of Surface Conductivity in Diamond. Physical Review Letters 2000;85(16):3472–5. [PubMed: 11030924]
26. Docheva D, Popov C, Mutschler W, Schieker M. Human mesenchymal stem cells in contact with their environment: surface characteristics and the integrin system. Journal of Cellular and Molecular Medicine 2007;11(1):21–38. [PubMed: 17367499]
27. Raffaini G, Ganazzoli F. Sequential adsorption of proteins and the surface modification of biomaterials: A molecular dynamics study. Journal of Materials Science: Materials in Medicine 2007;18(2):309–16. [PubMed: 17323163]
28. García AJ. Get a grip: integrins in cell–biomaterial interactions. Biomaterials 2005;26(36):7525–9. [PubMed: 16002137]
29. Lampin M, Warocquier–Clerout R, Legris C, Degrange M, Sigot-Luizard MF. Correlation between substratum roughness and wettability, cell adhesion, and cell migration. Journal of Biomedical Materials Research 1997;36(1):99–108. [PubMed: 9212394]
30. Garguilo JM, Davis BA, Buddie M, Kock FAM, Nemanich RJ. Fibrinogen adsorption onto microwave plasma chemical vapor deposited diamond films. Diamond and Related Materials 2004;13:595–9.
31. Sawyer AA, Hennessy KM, Bellis SL. The effect of adsorbed serum proteins, RGD and proteoglycan-binding peptides on the adhesion of mesenchymal stem cells to hydroxyapatite. Biomaterials 2007;28 (3):383–92. [PubMed: 16952395]
32. Haynes DR, Boyle SJ, Rogers SD, Howie DW, Vernon-Roberts B. Variation in cytokines induced by particles from different prosthetic materials. Clin Orthop Relat Res 1998;(352):223–30. [PubMed: 9678051]
33. Haynes DR, Rogers SD, Hay S, Pearcy MJ, Howie DW. The differences in toxicity and release of bone-resorbing mediators induced by titanium and cobalt-chromium-alloy wear particles. J Bone Joint Surg Am 1993;75(6):825–34. [PubMed: 8314823]
34. Faleiro C, Godinho I, Reus U, de Sousa M. Cobalt-chromium-molybdenum but not titanium-6aluminium-4vanadium alloy discs inhibit human T cell activation in vitro. Biometals 1996;9(4):321–6. [PubMed: 8837453]
35. Pypen CM, Dessein K, Helsen JA, Gomes M, Leenders H, De Bruijn JD. Comparison of the cytotoxicity of molybdenum as powder and as alloying element in a niobium-molybdenum alloy. J Mater Sci Mater Med 1998;9(12):761–5. [PubMed: 15348936]
36. Shanbhag ASJJ, Black J, Galante JO, Glant TT. Macrophage/particle interactions: effect of size, composition and surface area. J Biomed Mater Res 1994;28(1):81–90. [PubMed: 8126033]
37. Shanbhag ASJJ, Black J, Galante JO, Glant TT. Human monocyte response to particulate biomaterials generated in vivo and in vitro. J Orthop Res 1995;13(5):792–801. [PubMed: 7472759]

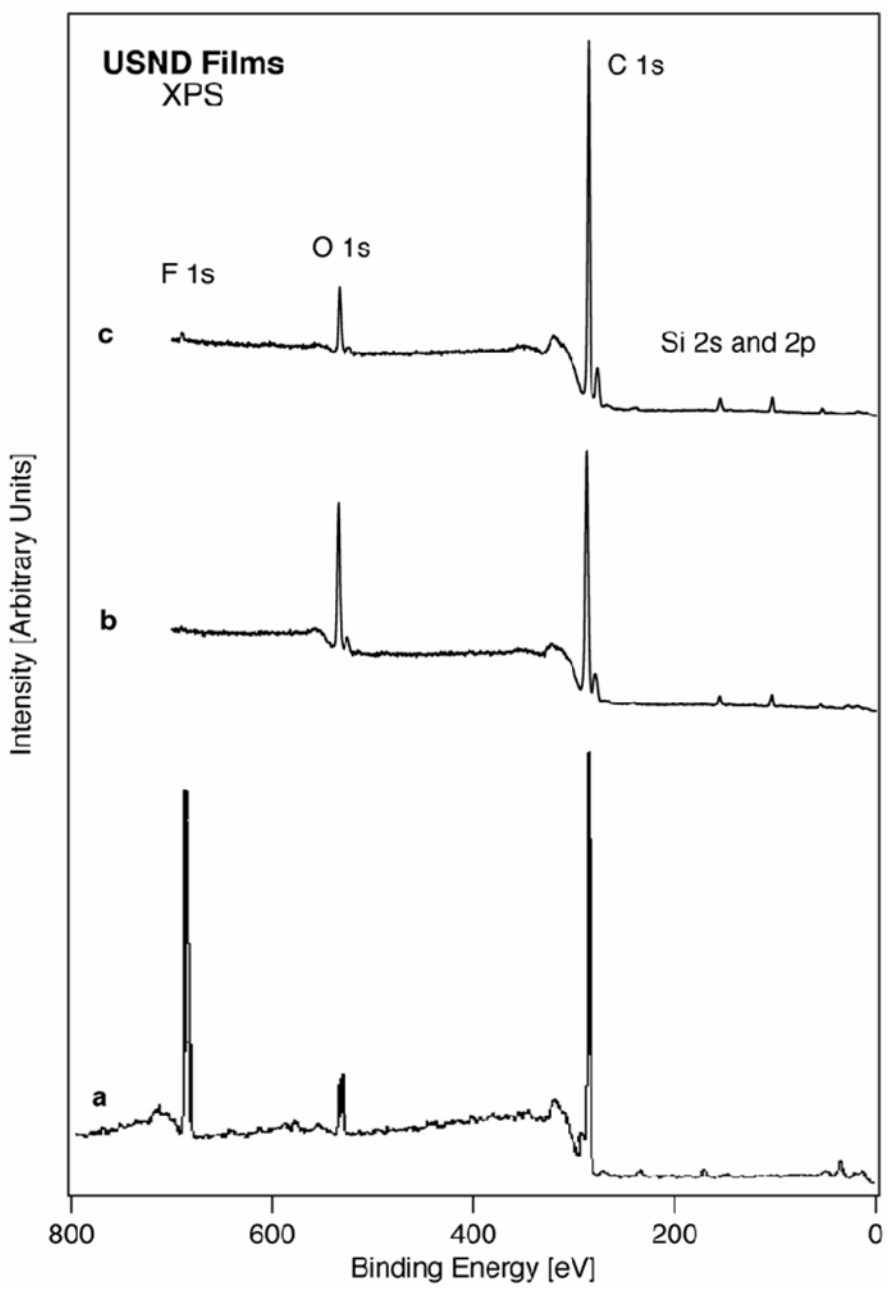

Figure 1.
XPS analysis of functionalized USND deposited on Ti-6Al-4V alloys. Survey spectrum of (a) F-terminated USND, (b) O-terminated USND, and (c) H-terminated USND.

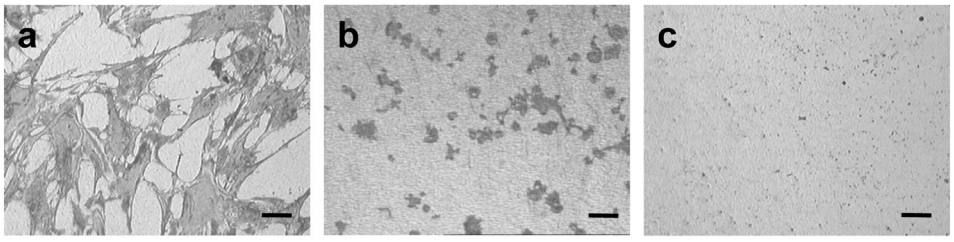

Figure 2.
Reflected light microscopy images demonstrating the morphology of MSCs cultured in serum-free DMEM for 1 hour on (A) H-terminated USND, (B) O-terminated USND, and (C) F-terminated USND. The cells readily attach to the H-terminated surface, while adhesion is very weak to the O-terminated or F-terminated surfaces. Scale bar = 100 μm.

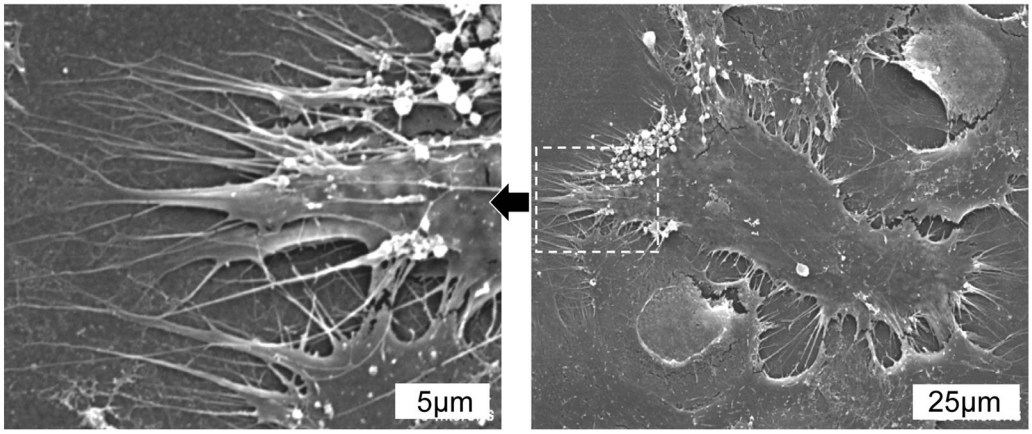

Figure 3.
SEM images of MSCs cultured for 24 hours on H-terminated USND. The image on the left shows a higher magnification of the area indicated in the right image. The cells adopt a spread morphology and extend many pseudopodia along the surface.

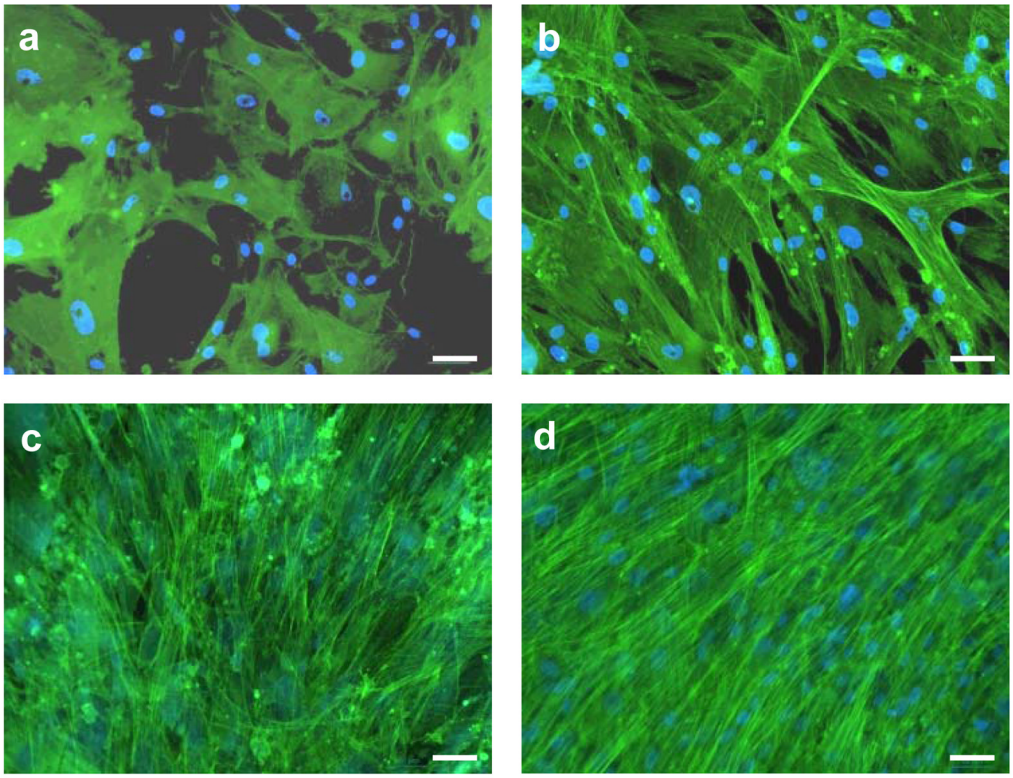

Figure 4.
Florescent images showing morphology of MSCs cultured for up to 2 weeks on H-terminated USND coatings. The cells were cultured on a USND surface for (a) 3 hours, (b) 24 hours, (c) 7 days, and (d) 14 days. MSCs readily attach, spread, and eventually form a confluent layer on this surface. Scale bar = 50 μm.

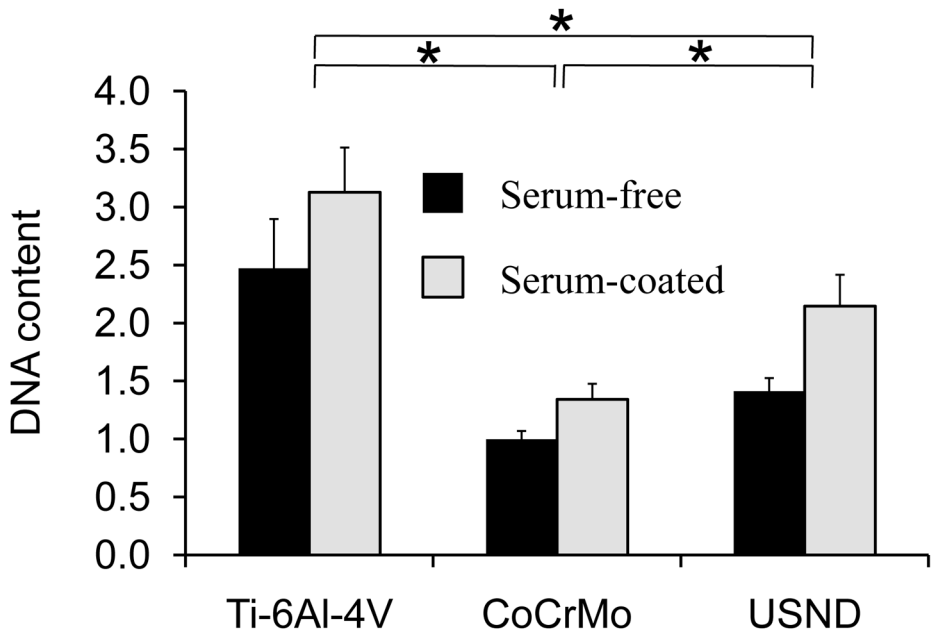

Figure 5.

Quantitative analysis of MSC adhesion to H-terminated USND, Ti-6Al-4V and CoCrMo. Prior to cell seeding, the surfaces were either pre-coated with serum (FBS) or left uncoated. Cells were cultured for 90 min, followed by mechanical agitation to remove loosely-bound MSCs. Remaining attached cells were quantified by assay for DNA content. Adhesion of MSCs to USND was found to be intermediate between that of Ti-6Al-4V and CoCr, in both serum-free conditions and in the presence of serum. * denotes $p < 0.05$

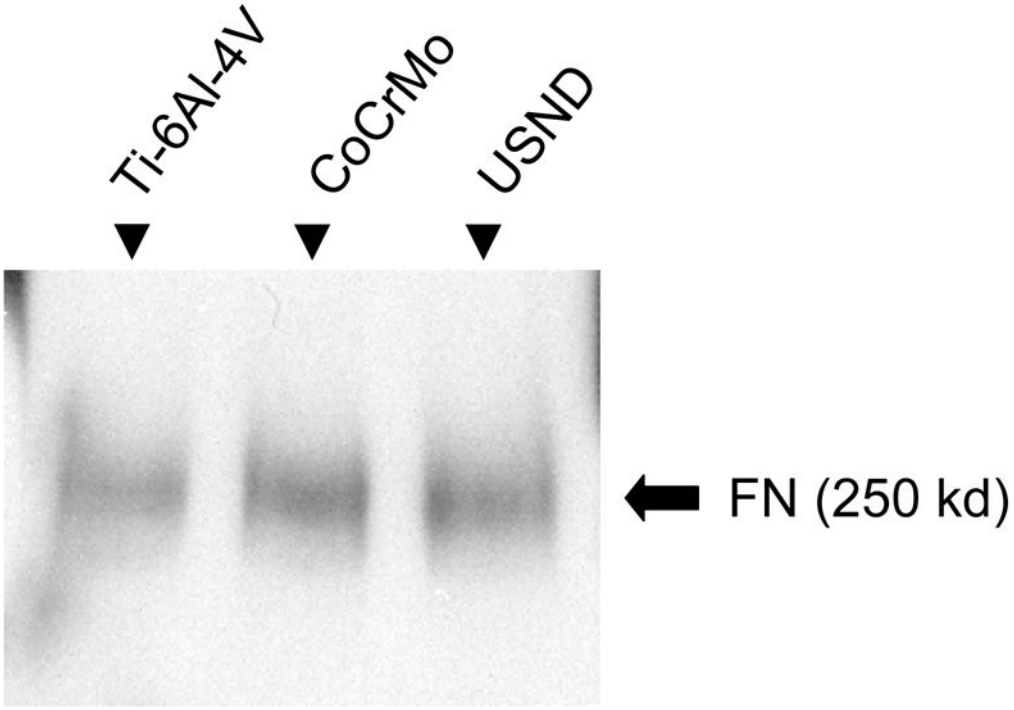

Figure 6.
Western blot for total fibronectin adsorbed to material surfaces. Similar amounts of fibronectin were deposited from serum (FBS) onto H-terminated USND, Ti-6Al-4V and CoCrMo substrates.

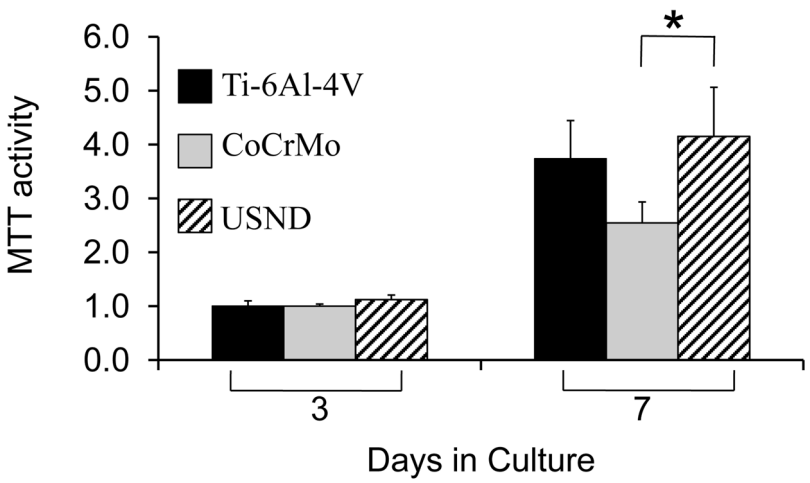

Figure 7.

Proliferation assay to assess potential long-term effects of exposure to USND on cell behavior. A small number of MSCs was seeded onto H-terminated USND, Ti-6Al-4V, or CoCrMo and cultured for up to one week. The number of viable cells was quantified at day 3 and 7 by an MTT assay. Cell proliferation on USND was not significantly different from Ti-6Al-4V, but was greater than that observed for cells grown on CoCrMo. * denotes $p < 0.05$

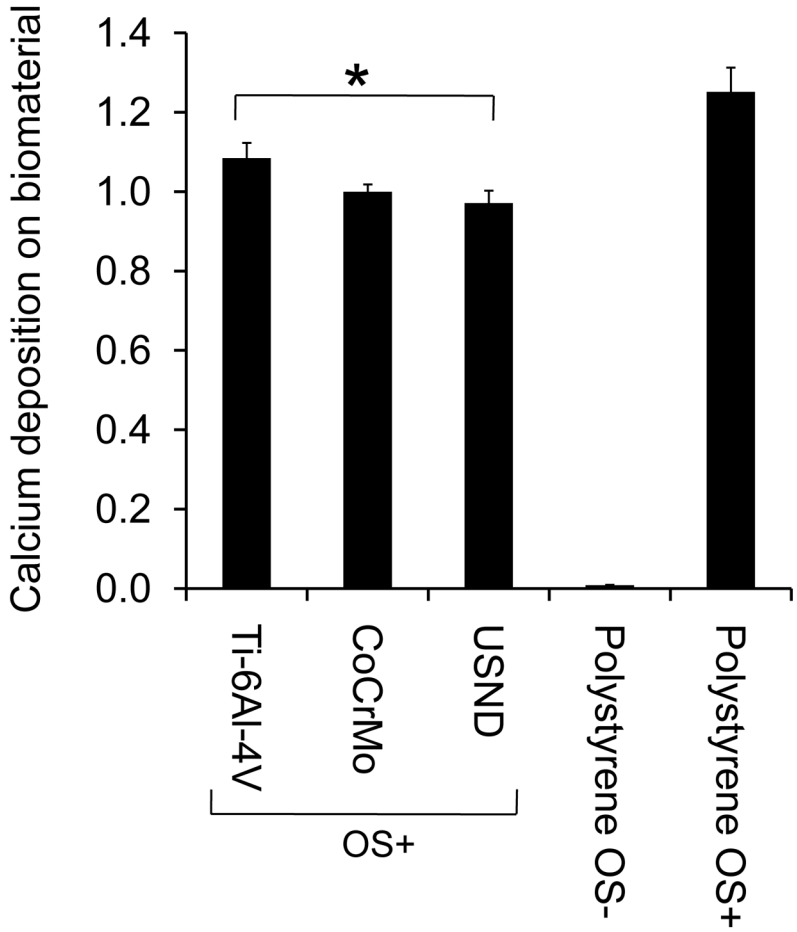

Figure 8.

Analysis of mineralized matrix deposited on H-terminated USND, Ti-6Al-4V and CoCrMo. Osteoblastic differentiation of MSCs adherent to the metal substrates was induced by culture for 4 weeks in an osteogenic media (OS+). The cells were allowed to deposit mineral on the biomaterial surfaces, and then the calcium content was quantified at week 4. Cells were also cultured on tissue culture plastic in osteogenic media (OS+, positive control) or in normal growth media (OS-, negative control). Slightly more mineral was deposited on Ti-6Al-4V than USND, but the difference in mineral deposition between USND and CoCrMo surfaces was not significant. * denotes $p < 0.05$

Table 1

Termination	O/C	F/C	OH/COO	C=O/C-C	Contact angle
H	0.08	--	0.10	0.19	86
O	0.21	--	1	1	<2
F	0.07	0.26	1.6	0.06	84

Relative composition ratios determined by XPS (mol%/mol%) and water contact angles determined on samples for each type of treatment. The O/C and F/C ratios were measured from survey scans in Figure 1. The hydroxyl to carbonate and carbonyl to aliphatic ratios were determined from high resolution XPS spectra of the O 1s and C 1s peaks for each sample. Relative uncertainties are expected to be around +/− 10% in each case. Contact angles were measured from one analysis on each type of sample.